Journal of Plant Interactions

ISSN: (Print) (Online) Journal homepage: https://www.tandfonline.com/loi/tjpi20

Formate dehydrogenase takes part in molybdenum and iron homeostasis and affects dark-induced senescence in plants

Irene Murgia , Gianpiero Vigani , Dario Di Silvestre , Pierluigi Mauri , Rossana Rossi , Andrea Bergamaschi , Miriam Frisella & Piero Morandini

To cite this article: Irene Murgia , Gianpiero Vigani , Dario Di Silvestre , Pierluigi Mauri , Rossana Rossi , Andrea Bergamaschi , Miriam Frisella & Piero Morandini (2020) Formate dehydrogenase takes part in molybdenum and iron homeostasis and affects dark-induced senescence in plants, Journal of Plant Interactions, 15:1, 386-397, DOI: 10.1080/17429145.2020.1836273

To link to this article: https://doi.org/10.1080/17429145.2020.1836273

JOURNAL OF PLANT INTERACTIONS
2020, VOL. 15, NO. 1, 386–397
https://doi.org/10.1080/17429145.2020.1836273

Formate dehydrogenase takes part in molybdenum and iron homeostasis and affects dark-induced senescence in plants

Irene Murgia [a], Gianpiero Vigani [b], Dario Di Silvestre [c], Pierluigi Mauri [c], Rossana Rossi [c], Andrea Bergamaschi [c], Miriam Frisella[a] and Piero Morandini [d]

[a]Biosciences Dept., University of Milano, Milano, Italy; [b]Plant Physiology Unit, Life Sciences and Systems Biology Dept., University of Torino, Torino, Italy; [c]Proteomic and Metabolomic Laboratory, ITB-CNR, Segrate, Italy; [d]Environmental Science and Policy Dept., University of Milano, Milano, Italy

ABSTRACT

Formate is produced, in plants, by various biochemical pathways and it is degraded by Formate Dehydrogenase FDH, in presence of NAD^+, into CO_2 and NADH. FDH has been proposed as one of the enzymes regulating molybdenum (Mo) and iron (Fe) homeostasis. Here we explored the impact of FDH perturbation on Mo and Fe plant nutritional status and FDH relevance on the plant responses against abiotic stresses, by using *in silico* and experimental approaches. The characterization of different *Arabidopsis thaliana* and *Nicotiana tabacum* FDH transgenic lines suggests that FDH promoter activity is dependent on both Mo and Fe nutritional supply and that FDH overexpression alters Mo concentrations in seeds and Fe concentration in seeds, leaves and stems. Also, FDH overexpression delays the dark-induced senescence whereas the lack of FDH accelerates its progression. FDH is therefore a multifaceted enzyme with impact on Mo and Fe homeostasis and regulation of dark-induced senescence.

ARTICLE HISTORY
Received 20 July 2020
Accepted 8 October 2020

KEYWORDS
Arabidopsis thaliana; *dark-induced senescence*; *formate dehydrogenase*; *iron*; *molybdenum*; *Nicotiana tabacum*

Introduction

Iron (Fe) and Molybdenum (Mo) are essential micronutrients for plants; the net of interactions and reciprocal homeostatic controls between Fe and Mo plant nutritional status involve Mo-dependent enzymes, Fe and Mo transport and their intracellular trafficking (Baxter et al. 2008b; Baxter 2009; Bittner 2014; Murgia and Vigani 2015; Vigani et al. 2017). The physiological and biochemical effects of combined Mo and Fe starvation were recently investigated in *Cucumis sativus*, together with the changes in the ionomes and proteomes of their Mo and/or Fe-deficient root mitochondria; in particular, the high-throughput profiling of the mitochondrial proteomes through the Multidimensional Protein Identification Technology (MudPIT) identified more than a hundred differentially expressed proteins under the various Mo and Fe nutritional supply (Vigani et al. 2017). The NAD^+-dependent enzyme formate dehydrogenase (FDH) was proposed as one of the key proteins regulating Fe and Mo homeostasis (Vigani et al. 2017).

Formate can be produced during various plant metabolic pathways, such as the detoxification of formaldehyde by GSH (Achkor et al. 2003; Song et al. 2013), as well as during the Methionine (Met) cycle (Vigani et al. 2017 and references therein).

FDH is present in bacteria, fungi and plants and catalyses the reversible reaction: $NAD^+ + HCOOH \leftrightarrow NADH + H^+ + CO_2$. The reduction of CO_2 to formate catalysed by FDH takes place in some bacteria and it is considered an attractive approach for carbon fixation (Maia et al. 2016; Cotton et al. 2018). However, the reduction of CO_2 is not favored in normal conditions in plants, as the standard transformed Gibbs energy of the reaction ($\Delta_rG'°$, used for biochemical reactions, see Alberty et al. 2011) is around +15 kJ mol^{-1} (Cotton et al. 2018) at pH 7.0 and at ionic strength of 0.25 (the physiological total ion concentration) (Alberty et al. 2011).

In plants, FDH is a phosphoprotein that can be ubiquitinated by the RING-type ubiquitin ligase Keep-on-Going KEG which controls FDH turnover via proteasome-degradation (McNeilly et al. 2018); FDH is localized in mitochondria and chloroplasts (Herman et al. 2002; Choi et al. 2014) and its expression is induced by formate as well as its reduced forms formaldehyde and methanol (Hourton-Cabassa et al. 1998; Fukusaki et al. 2000; Li et al. 2001). Notably, FDH could act as mediator of plant response against biotic and abiotic stresses, depending on its phosphorylation and ubiquitination status (Hourton-Cabassa et al. 1998; Choi et al. 2014; McNeilly et al. 2018).

A functional role for FDH during stress is still sought; for instance, formate itself might act as protectant during photoinhibition (Shiraishi et al. 2000), but no conclusive evidence for its role as an *in vivo* scavenger of ROS is available, so far.

A. thaliana atfdh insertional mutants manifested enhanced disease symptoms upon infection with avirulent *Pseudomonas syringae* pv *tomato* Pst DC3000 (avrRpm1); such a finding led to the general hypothesis that FDH could play a role in the regulation of defence responses against bacterial pathogens (Choi et al. 2014).

Besides FDH, other enzymes are involved in the metabolism of formate in plant cells; however, the metabolic interactions between formate degradation via FDH and other formate catabolic pathways, such as its coupling to tetrahydrofolate (THF) for the entry into C1 metabolism with production of 10-formyl-tetrahydrofolate (Prabhu et al. 1996; Song et al. 2013), are uncertain.

CONTACT Irene Murgia irene.murgia@unimi.it Biosciences Dept., University of Milano, via Celoria 26, 20133, Milano, Italy
Supplemental data for this article can be accessed https://doi.org/10.1080/17429145.2020.1836273

The aim of this work is to validate the hypothesis that FDH takes part in the modulation of Mo and Fe homeostasis (Vigani et al. 2017); such a hypothesis is supported by various evidences among which the opposite behavior displayed by FDH protein levels in *C. sativus* root mitochondria in plants grown under Mo or Fe deficiency (Vigani et al. 2017). Such results are particularly interesting, given the FDH ancillary role in the Met cycle with the biosynthesis of the Fe chelator nicotianamine for phloematic Fe transport and distribution (Miyazaki and Yang 1987; Kobayashi et al. 2005; Kobayashi and Nishizawa 2012; Itai et al. 2013). Notably, plant FDH, as opposed to its bacterial counterpart, does not require the Mo cofactor Moco in its active site; nonetheless, an indirect regulation of plant FDH by Mo was suggested as part of the proposed model of Fe and Mo homeostatic interactions in root mitochondria (Vigani et al. 2017).

Moreover, we also intended to explore FDH role during abiotic stresses; although FDH has been already known as 'stress-responsive' enzyme (Alekseeva et al. 2011), the putative impact of FDH on Fe homeostasis suggested us to investigate its role on those abiotic stresses for which the relevance of Fe homeostasis has been established, such as the demonstrated impact of the Fe-storage ferritin during senescence and dark-induced senescence (Tarantino et al. 2003; Murgia et al. 2007; Briat et al. 2010)

We therefore first applied transcript correlation analysis, an *in silico* approach which can successfully assist the assignment of a given candidate gene to a metabolic pathway, as occurred for *A. thaliana* CYP82C4 gene coding for a P450 enzyme and involved in Fe metabolism (Murgia et al. 2011). CYP82C4 indeed catalyzes the last biosynthetic step of sideretin released from roots as a general strategy for iron acquisition (Rajniak et al. 2018).

Furthermore, we explored the role of FDH by using *Arabidopsis thaliana* and *Nicotiana tabacum* as model plants; in particular, we analysed *A. thaliana* and *N. tabacum* FDH transgenic plants at various Mo and Fe nutritional conditions and after exposure to abiotic stresses. Taken together, obtained results indicate that plant FDH is a multifaceted enzyme which depends on Mo and Fe nutrition and acts itself as part of Mo and Fe homeostasis and as a link between plant nutrition and senescence.

Material and methods

Transcript correlation analysis

Transcript correlation analysis was performed as described previously (Menges et al. 2008; Murgia et al. 2011); the dataset used for such analysis is described in (Menges et al. 2008).

Seed Sterilization

A. thaliana seeds were sterilized as described in (Murgia et al. 2015). *N. tabacum* seeds were sterilized by soaking them 2 hrs in 2% Tween 20 in water, the solution was replaced with a solution of 2% Tween 20 in commercial sodium hypochlorite; seeds were then vortexed vigorously for 10 min, the solution was removed and commercial sodium hypochlorite was added for another 30 min; seeds were then rinsed six times with sterile water.

Growth of A. thaliana *and* N. tabacum

Plant growth in soil: *A. thaliana* wt Col, *atfdh1-5* Salk_108751-1 (N869258) (wt Col) (Alonso et al. 2003; Choi et al. 2014), and *A. thaliana* transgenic line transformed with the construct of *Vigna umbellata* FDH promoter fused to the reporter GUS (*Vu* FDH::GUS in short) (Lou et al. 2016) were grown in either control or alkaline soil as described in (Murgia et al. 2015). *N. tabacum* (Lou et al. 2016) was grown, unless differently specified, at 25°C, 100 μE m^{-2} s^{-1} 14 h:10 h light:dark on Technic nr.1 DueEmme soil.

Plant growth in vitro: *A. thaliana* was grown on AIS medium as described in (Murgia et al. 1998); Mo was supplemented as ammonium molybdate, whereas Fe was supplemented as Fe(III)EDTA. Mo and Fe nutritional conditions: control (0.2 μM Mo, 50 μM Fe), Mo deprivation (0 μM Mo, 50 μM Fe), Mo excess (10 μM Mo, 50 μM Fe), Fe deficiency (0.2 μM Mo, 5 μM Fe), Fe excess (0.2 μM Mo, 500 μM Fe) or Mo deprivation and Fe deficiency (0 μM Mo, 5 μM Fe), unless otherwise specified.

N. tabacum was grown on Hoagland medium (1x Hoagland nr. 2 basal salt mixture Sigma 2395), 2% sucrose, 0.8% plant agar, pH adjusted at 5.8 with NaOH. When indicated, formate was supplemented as $KHCO_2$.

GUS staining

GUS staining of seeds and young seedlings was performed as in (Murgia et al. 2015). All other tissues were stained as in (Elorza et al. 2004).

PCR

T-DNA insertion in the *atfdh1-5* mutant SALK 108751 (Alonso et al. 2003; Choi et al. 2014) is localized in the third exon of FDH gene At5g14780 and homozygosity was confirmed by PCR, with following primers: FDH-1F: GGCATCTTCTGGTGATAGCA, FDH-2R: ATGATCCGAGCCAATACCAG; FDH-3F: CAACGTGGTCTCAG TGGCAG; FDH-4R: ATGGTGGTGCCGGAGGTATG; LBa1: TGGTTCACGTAGTGGGCCATCG. All the PCR were performed as follows: first denaturation at 94°C/90 s, then 35 cycles at 93°C/50 s, 58°C/60 s and 72°C/60 s, and a final elongation at 72°C/300 s.

Photoinhibition and photochemical parameters

Leaf disks were cut from second and third youngest leaves from 4 weeks old *N. tabacum* plants and placed on plates containing 1 mM K_2SO_4, 0.1 mM $CaSO_4$, 10 mM NaP medium, 0.75% plant agar at pH 7.0, photoinhibited at 800 μE $m^{-2}s^{-1}$ light, up to 8 h and then maintained 4 h at 100 μE m^{-2} s^{-1} light, for recovery. Leaves cut from rosettes of 3 weeks old *A. thaliana* plants were floated 90 min in the dark, in either H_2O or 1 mM lincomycin, and photoinhibited as described above.

Total chlorophyll content (Chla + Chlb) was measured as described (Tarantino et al. 2003, 2005). The photochemical parameters F_0, F_m, F_v/F_m were calculated by evaluating chlorophyll fluorescence with a portable plant efficiency analyzer (Hansatech Instruments, Norfolk, UK), as described (Tarantino et al. 2003, 2005). Statistical analyses of total Chl content, F_0, F_m, were performed with χ^2 test; statistical

analysis of F_v/F_m was performed with T-Test (given the range of F_v/F_m values).

Enriched mitochondrial fraction

Around 40 g of *N. tabacum* leaves from 10 weeks old plants were harvested (from youngest leaf, considered as leaf nr.1 up to leaf nr.9), rinsed in cold deionized water, briefly dried on absorbing paper and then chopped in a mixer with 150 ml cold extraction buffer EB, 5x spins, 2 s each. The suspension was gently filtered on 4 layers of Miracloth and the collected leaf fragments were chopped on the mixer, with cold 50 ml EB, 2x spins of 2 s each, and filtered again. The procedure of collecting leaf fragments was then repeated, cell debris was pelleted by centrifugation 5 min at 2000 g, the supernatant was centrifuged 10 min at 16000 g; the pellet was gently resuspended in washing buffer WS (with a thin paintbrush) and centrifuged 15 min at 11000 g. This last step was repeated twice and then the pellet was resuspended in 650 µl WB for further analyses. EB: 0.45 M sucrose, 15 mM MOPS, 1.5 mM EGTA pH 7.4 with KOH; added before use: 0.6% polyvinylpyrrolidone (PVP), 0.2% (w/v) BSA, 10 mM DTT and 0.2 mM phenylmethylsulfonyl fluoride (PMSF). WB: 0.3 M sucrose, 10 mM MOPS, 1 mM EGTA, pH 7.2 with KOH; added before use: 0.2 mM PMSF.

Sample preparation for proteomic analysis

The enriched mitochondrial fraction was centrifuged at 12000 g for 20 min and treated with RapiGest SF (Waters Corporation, Milford, MA, USA) at 0.25% (w/v) final concentration. After incubation at 100°C for 20 min, the samples were cooled to room temperature and centrifuged 10 min at 2200 g. The protein concentration was assayed using the SPN™ Protein Assay kit (G-Biosciences, St. Louis, MO, USA) and 50 ± 0.5 µg protein from each sample was digested with Sequencing Grade Modified Trypsin (Promega, Madison, WI, USA) using a 1:50 (w/w) enzyme/substrate ratio at 37°C overnight. Then, an additional aliquot of enzyme was added at an enzyme/substrate ratio of 1:100 (w/w) and the digestion continued for 4 h. The enzymatic reaction was chemically stopped by acidification with 0.5% trifluoroacetic acid (Sigma-Aldrich Inc., St. Louis, MO, USA), followed by incubation at 37°C for 45 min and 10 min centrifugation at 13000 g to remove hydrolytic RapiGest SF by-products. Samples were then desalted by Pierce™ C-18 spin columns (Thermo Fisher Scientific, Waltham, MA, USA), concentrated in a SpeedVac (Savant Instruments Farmingdale, NY, USA) at 60°C and resuspended in 0.1% formic acid (Sigma-Aldrich Inc., St. Louis, MO, USA) at 1 µg μL^{-1}.

Nano-LC–MS/MS

Trypsin-digested mixtures were resolved by the Eksigent nano LC-Ultra 2D System (Eksigent, AB SCIEX Dublin, CA, USA) and analysed by LTQ-OrbitrapXL-ETD mass spectrometer (Thermo Fisher Scientific, San José, CA, USA), equipped with a nanospray ionization source (Thermo Fisher). Chromatographic and mass spectrometry were performed as described in (Vigani et al. 2017).

Element analyses *in* N. tabacum

First and second youngest *N. tabacum* leaves (of at least 8 cm in length) and stems were sampled from 10 weeks old plants, whereas their seeds were collected from ripened seed capsules. Leaves, stems and seeds were dried at 100°C, mineralized and the concentrations of various elements were measured by inductively coupled plasma mass spectrometry (ICP-MS) as in (Islam et al. 2020); the statistical analyses were performed according to (Martin-Sanchez et al. 2020).

Results

FDH expression correlates with chloroplastic activities

Correlation analysis of *A. thaliana* FDH transcript was performed over the entire genome (Table S1). Surprisingly, most of the genes with highest Pearson's correlation coefficient with FDH in the logarithmic space (Table 1) encode chloroplastic proteins with transmembrane domains, according to plant database Aramemnon (Schwacke et al. 2003) (http://aramemnon.uni-koeln.de). YLMG1-2 is a close homolog of YLMG1-1, involved in chloroplast biogenesis (Kabeya et al. 2010; Chen et al. 2018). A maize ortholog of *A. thaliana* YLMG1-2 is localized in proplastids, however not in considerable amounts in the chloroplastic DNA–protein conglomerates named nucleoids; its involvement in the anchoring or the distribution of the nucleoids is still uncertain (Majeran et al. 2012; Oldenburg and Bendich 2015). YCF36 is a protein of unknown function but related to

Table 1. Top correlators of *A. thaliana* FDH transcript in logarithmic analysis.

Accession number	Annotation	Pearsons's coefficient (in log)	Localization	Transmembrane domain
AT5G14780	FDH	1	mitochondria, chloroplast	no
AT4G27990	YLMG1-2	0.7487	chloroplast	yes
AT5G11840	YCF36	0.7102	chloroplast	yes
AT2G20920	CRS	0.6969	chloroplast	yes
AT3G21790	UGT71B7	0.689	cytosol	no
AT4G13250	NYC1	0.6776	chloroplast	yes
AT3G44880	PAO	0.6717	chloroplast	yes
AT2G24860	DNAJ/HSP40	0.6675	chloroplast	no
AT3G26170	CYP71B19	0.6638	secretory pathway	yes
AT1G10500	ISCA1/SUFA	0.6631	chloroplast	no
AT3G48740	SWEET1	0.6571	secretory pathway	yes
AT3G26580	TCP34	0.6514	chloroplast	yes
AT4G19390	unknown function	0.6498	chloroplast	yes

Note: The genes are listed together with their respective *Pearson*'s correlation coefficients, from log analysis. Putative intracellular localization and presence of transmembrane domains are according to Aramemnon database (http://aramemnon.uni-koeln.de/).

ORF which are present in the plastid genome of various photosynthetic algae (Douglas and Penny 1999; Urzica et al. 2012). The cell growth defect factor-related protein CRS promotes plant senescence (Cui et al. 2013). Uridine diphosphate glucosyltransferase UGT71B7 is involved in ABA homeostasis (Dong et al. 2014). Pheophorbide a Oxygenase PaO and Chlorophyll b Reductase NYC1 (Non-Yellow Coloring 1) are involved in chlorophyll catabolism which occurs, in physiological conditions, during leaf senescence and fruit ripening in chloroplasts. Chlorophyll catabolism consists of various steps acting in cascade (Hörtensteiner and Kräutler 2011; Hörtensteiner 2013; Kräutler 2016). NYC1 is part of the chlorophyll cycle regulating the Chl a/Chl b ratio and the reduction of Chl b to Chla (Jia et al. 2015). DNAJ/HSP40 is part of the dynamic complexes associated with MAMPs-triggered immunity MTI (Mishra et al. 2017). CYP71B19 expression is induced in response to ABA, IAA and osmotic stress (Schuler et al. 2006). IscA, a component of the SUF system of Fe-S cluster biosynthesis in chloroplasts, can act as scaffold protein although its role in *A. thaliana* seems, so far, not essential (Abdel-Ghany et al. 2005; Yabe and Nakai 2006; Balk and Pilon 2011; Couturier et al. 2013). SWEET11 is a sucrose exporter for phloem loading (Chen et al. 2012); it is also expressed in cells associated with xylem vessels and it can transport also glucose and fructose (Le Hir et al. 2015). TCP34 (tetratricopeptide-containing chloroplast protein of 34 KDa) can bind plastidic DNA (Weber et al. 2006; Kabeya et al. 2010; Majeran et al. 2012; Pfalz and Pfanneschmidt 2013).

Most of the genes with highest Pearson's correlation coefficient with FDH in the linear analysis also encode chloroplastic proteins, some of which contain transmembrane domains (Table S2); AAE3 is a cytosolic oxalyl CoA synthetase required for the catabolism of oxalate into CO_2, with formate as a probable intermediate (Foster et al. 2012). RSH3 is homologous of the bacterial RelA/SpoT which determine the levels of the effectors of the 'stringent response,' i.e. of guanosine tetraphosphate ppGpp and guanosine pentaphosphate pppGpp (van der Biezen et al. 2000). Remarkably, (p)ppGpp regulates chloroplast gene expression and breakdown during both dark-induced and developmental senescence, as well as nutrient remobilization (Sugliani et al. 2016). EBF2 modulates ethylene perception (Binder et al. 2007). AIM1 is required for the production of benzoylated metabolites (Bussell et al. 2014). PED1 is a 3-ketoacyl-CoA thiolase involved in the fatty acid degradation and ABA signaling (Burkhart et al. 2013); BCM2 promotes chlorophyll homeostasis during leaf senescence (Wang et al. 2020).

FDH promoter activity is dependent on plant Mo and Fe availability

An *A. thaliana* transgenic line carrying a *Vigna umbellata* (rice bean) FDH promoter::GUS construct (Vu FDH::GUS) (Lou et al. 2016) was grown in AIS medium at various Mo or Fe concentrations, i.e. control, Mo deprivation, Mo excess, Fe deficiency, Fe excess, or Mo deprivation and Fe deficiency. Mo deprived seedlings show longer roots (Figure S1(A)), in agreement with what observed in *C. sativus* grown under Mo deficiency (Vigani et al. 2017); longer Vu FDH::GUS roots are however observed also under Mo deprivation and Fe deficiency (Figure S1(A)), differently from *C.sativus* roots whose growth is inhibited by dual deficiency (Vigani et al. 2017). Mo excess, Fe deficiency and Fe excess all cause a reduction in root length (Figure S1(A)); Mo excess, Fe deficiency or Mo deprivation and Fe deficiency cause a decrease in chlorophyll concentration (Figure S1(B)). FDH promoter activity was detected in the vascular cylinder of roots, hypocotyls, petioles, leaves, trichomes and hydatodes of control seedlings (Figure 1(A)); a decrease of FDH promoter activity under Mo deprivation (Figure 1(B)) and an increase under Mo excess (Figure 1(C)) was observed in the various seedlings inspected for each nutritional condition. Also, FDH promoter activity increases, mainly at the shoot level, under perturbation of Fe availability, i.e. Fe deficiency (Figure 1(D)) and Fe excess (Figure 1(E)); however, Mo nutritional status dominates on Fe nutritional status in the regulation of FDH promoter activity, since Mo deprivation can reduce such activity, also under Fe deficiency (Figure 1(F)).

The dependence of FDH promoter activity on Mo and Fe supply was also tested on progeny seedlings from plants grown in vitro at altered Mo or Fe availability. For that, seeds collected from *Vu* FDH::GUS plantlets grown in vitro in control condition (0.2 μM Mo, 50 μM Fe), Mo deprivation (0 μM Mo, 50 μM Fe), Mo excess (5 μM Mo, 50 μM Fe), Fe deficiency (0.2 μM Mo, 5 μM Fe) were germinated on water-soaked paper and stained for GUS activity. After 24 h, FDH promoter activity is detected in Mo-excess and Fe-deficiency seeds (Figure 2). After three days, such activity is detected in the cotyledons of all analysed seedlings (Figure 3 (A–D)) as well as in the hypocotyl and roots of control and Mo-excess seedlings (Figure 3(A, C)); notably, intensity of the staining is directly correlated with Mo concentration (Figure 3(A–C)). After ten days (Figure 3(E–H)), a faint GUS staining is detected in control seedlings whereas GUS staining is still clearly visible in Mo-excess seedlings, in their cotyledons, root vascular cylinder and tips (Figure 3(G)).

FDH promoter activity was analysed also in *Vu* FDH::GUS *A. thaliana* plants grown in control (Figure S2), or in calcareous soil at pH 7.7 causing Fe deficiency (Figure S3); a higher variability of GUS staining was observed, when compared with growth in vitro; in any case, control plants show a diffuse GUS staining in leaves and particularly at leaf margins and hydathodes (Figure S2). FDH promoter activity can also be detected at petioles, leaf vasculature and hydathodes of plantlets grown in calcareous soil (Figure S3).

FDH overexpression alters Fe and Mo plant content

N. tabacum FDH lines overexpressing *V. umbellata* FDH (line1 and line2) (Lou et al. 2016) (for short named OE1 and OE2 from now onwards) accumulate less formate than wt, during the stress response induced by exposure to aluminium (Lou et al. 2016). According to the authors, exogenous formate application results in a dose-dependent inhibition of root elongation (Lou et al. 2016); we therefore treated FDH OE1 and OE2 tobacco plants with 0.4 M formate to verify if FDH overexpression could alter such inhibitory effect of exogenous formate on root elongation; we confirmed inhibitory effect of 0.4 mM formate on root elongation, however all treated lines showed same root length, regardless of FDH overexpression (Figure S4). Due to lack of information about FDH protein levels in OE1 and OE2 (Lou et al. 2016), overexpression of FDH was therefore first analysed by Multidimensional Protein Identification Technology (MUD-Pit) in enriched mitochondrial fractions prepared from OE1 and

OE2 leaves (Figure S5). OE1 and OE2 are genuinely overexpressing FDH, although only the native isoform could be detected, not the *V. umbellata* one, as shown by the peptide fragments identified by mass spectrometry during proteomic analysis (Figure S5).

Weights of OE1 and OE2 seedlings are higher than the corresponding wt values, both in control as well as under double Mo and Fe deficiency (Figure S6(A)), whereas chlorophyll contents of OE1 and OE2 seedlings are similar to wt ones, both in the single or double Mo and Fe nutritional deficiencies (Figure S6(B)). Notably, the chlorophyll content is slightly reduced in OE1 and OE2 seedlings grown under single Fe deficiency, with respect to wt in the same experimental condition (Figure S6(B)).

FDH overexpression consistently perturbs leaves and stems ionomes of OE1 and OE2 adult plant (10 weeks old) grown under control conditions as well as ionome of their mature seeds, collected from dry capsules of plants allowed to senesce in control growth conditions (Table 2); Fe is the most affected element, its content being reduced in OE1 and OE2 leaves, stems and seeds, whereas Mo content increases in OE1 and OE2 seeds. Other elements are also affected; indeed, Mg and Mn are increased in leaves and stems, Zn is decreased in leaves and increased in seeds, Cu is increased in seeds and Na is decreased in leaves and increased in stems, in OE1 and OE2 plants (Table 2).

FDH is involved in the onset of dark-induced senescence

The transcript correlation analysis shown above suggests an involvement of FDH in chlorophyll catabolism and in the onset of senescence. FDH role was therefore explored in photoinhibitory conditions associated with chlorophyll catabolism, and during natural or dark induced senescence, a condition in which the involvement of the Fe-storage protein

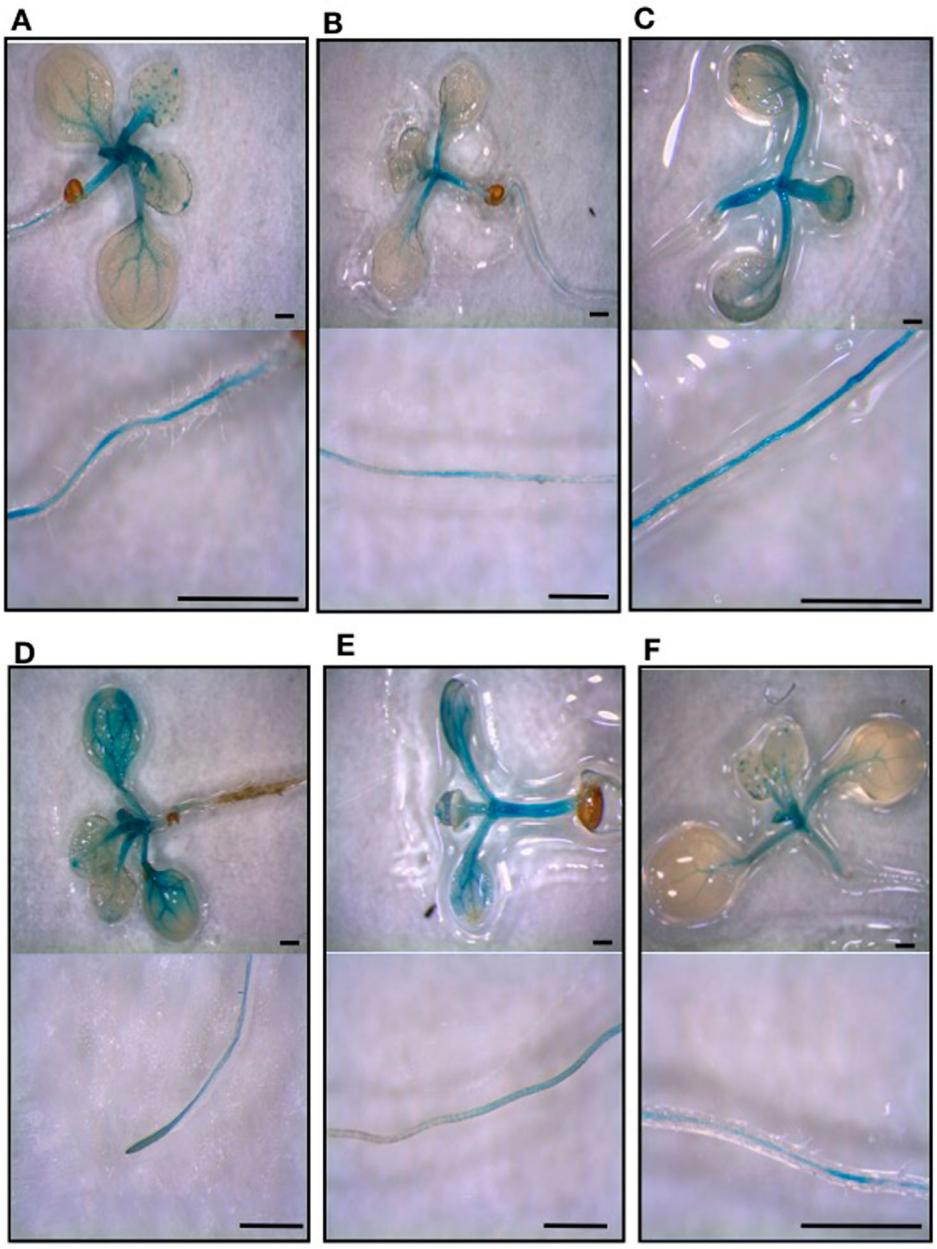

Figure 1. FDH promoter activity in seedlings grown at different Mo and Fe supply. *Vu*::GUS *A. thaliana* seedlings grown ten days in vitro on AIS medium, in square Petri dishes in upright position, at various Mo and Fe concentrations: **(A)** control (0.2 μM Mo, 50 μM Fe), **(B)** Mo deprivation (0 μM Mo, 50 μM Fe), **(C)** Mo excess (10 μM Mo, 50 μM Fe), **(D)** Fe deficiency (0.2 μM Mo, 5 μM Fe), **(E)** Fe excess (0.2 μM Mo, 500 μM Fe), **(F)** Mo deprivation and Fe deficiency (0 μM Mo, 5 μM Fe) were stained for β-Glucuronidase (GUS) activity. For each condition, aerial parts of the seedlings (upper panels) and their roots (lower panels) are shown. Bars = 1 mm.

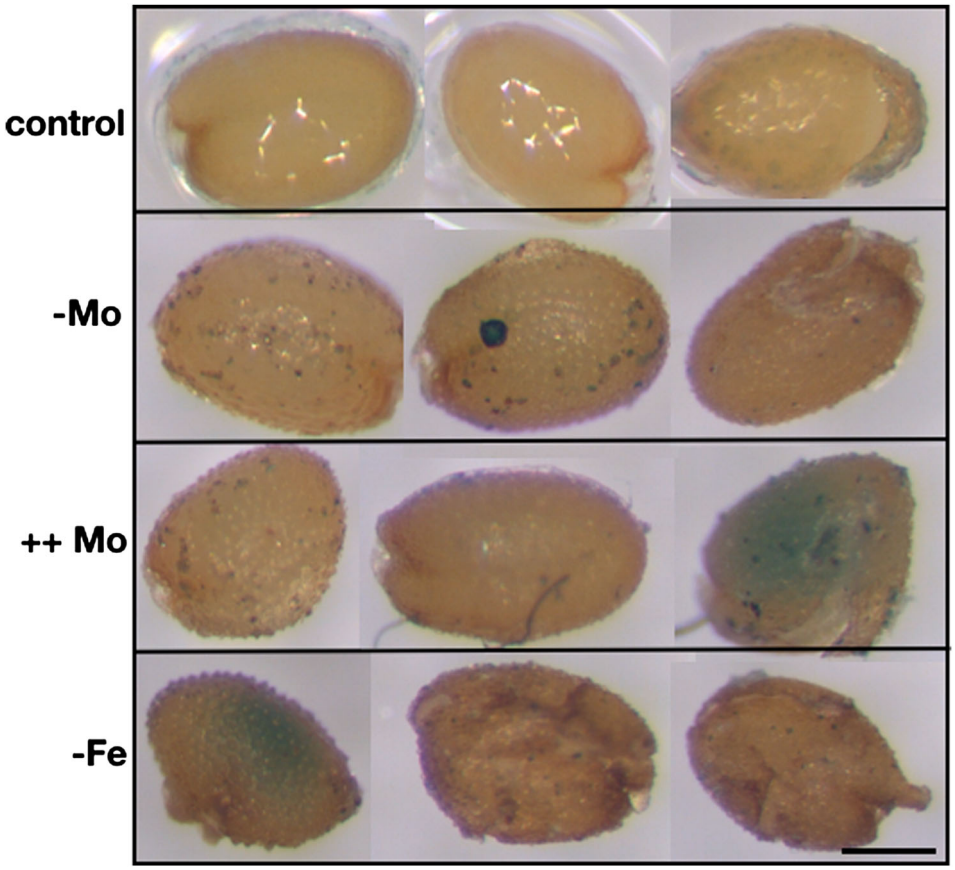

Figure 2. FDH promoter activity in *Vu* FDH::GUS *A. thaliana* seeds produced from plants grown in vitro at different Mo and Fe supply. *Vu* FDH::GUS *A.thaliana* seeds produced from plants grown in vitro on AIS medium at various Mo and Fe concentrations**:** control (0.2 µM Mo, 50 µM Fe), Mo deprivation (-Mo) (0 µM Mo, 50 µM Fe), Mo excess (++ Mo) (5 µM Mo, 50 µM Fe), Fe deficiency (-Fe) (0.2 µM Mo, 5 µM Fe) were maintained 24 h on water-soaked paper and then stained for β-Glucuronidase (GUS) activity. Bar = 200 µm.

ferritin regulating Fe homeostasis and trafficking has been fully established (Tarantino et al. 2003; Murgia et al. 2007; Briat et al. 2010).

Vu FDH::GUS *A. thaliana* plants were exposed to photoinhibitory conditions, i.e. at 800 µE m^2 sec^{-1} (Figure S7(A)); as expected, a reduction of maximal photochemical efficiency F_v/F_m was observed by exposure to high light, when compared to untreated plants (t0), especially in presence of the antibiotic lincomycin which blocks D1 turnover (Tyystjärvi and Aro 1996; Murata et al. 2012) (Figure S7(A)). An increase in FDH promoter activity could be occasionally observed along the margins of photoinhibited leaves (Figure

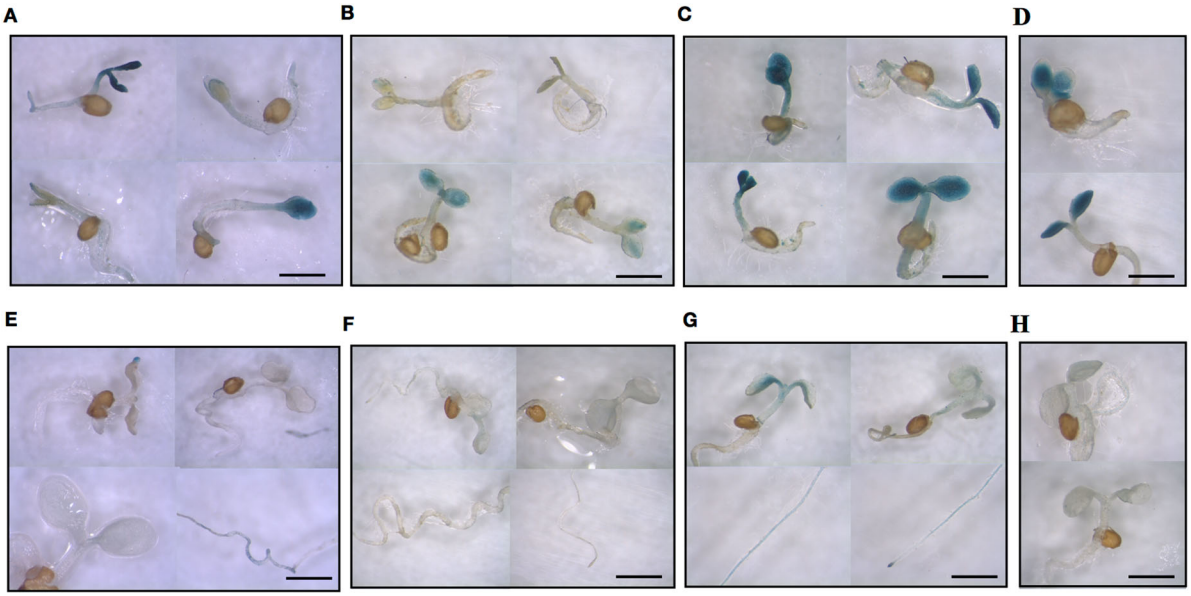

Figure 3. FDH promoter activity in *A. thaliana* progeny seedlings from plants grown in vitro at different Mo and Fe supply. *Vu*::GUS *A. thaliana* seeds produced from plants grown in vitro on AIS medium at various Mo and Fe concentrations were germinated on water-soaked paper and stained for GUS activity after **(A,B,C, D)** three or **(E,F,G,H)** ten days from germination; **(A, E)** control (0.2 µM Mo, 50 µM Fe); **(B, F)** Mo deprivation (0 µM Mo, 50 µM Fe); **(C, G)** Mo excess (5 µM Mo, 50 µM Fe); **(D,H)** Fe deficiency (0.2 µM Mo, 5 µM Fe). Bars = 1 mm.

Table 2. Elements profile of leaves, stems and seeds of *N.tabacum* wild type (wt) and FDH overexpressing lines OE1 and OE2.

	LEAVES			STEMS			SEEDS		
	wt	OE1	OE2	wt	OE1	OE2	wt	OE1	OE2
Na	1037.81**b**	476.18**a**	431.93**a**	337.24**a**	1701.07**b**	1468.08**b**	222.59a	149.46a	265.08a
	±498.89	±161.56	±171.3	±268.62	±528.92	±389.31	±95.39	±25.03	±20.86
Mg	22959.75**b**	8298.7**a**	9906.96**a**	7105.10**b**	1358.23**a**	1672.75**a**	5176.24a	5001.76a	5532.14a
	±8505.61	±885.547	±1642.55	±366.54	±126.4	±692.91	±377.689	±60.83	±254.17
Ca	4335.10**a**	24247.70**b**	25995.71**ab**	n.d	n.d.	n.d.	2158.66**a**	1867.24**a**	6011.62**b**
	±21337.60	±2375.38	±2983.33				±295.04	±241.60	±990.36
K	5600.40a	41799.4a	31118.41a	n.d	n.d.	n.d.	9146.08	9756.32	19500.1
	±5960.71	±3986.78	±3399.98				±575.54	±1137.6	±329.43
Mn	276.18**b**	150.31**a**	158.31**a**	40.97**b**	14.48**a**	17.51**a**	49.42a	50.32a	53.41a
	±17.13	±25.47	±19.09	±11.99	±3.43	±5.50	±2.31	±0.45	±2.24
Fe	344.06**b**	126.19**a**	157.12**a**	89.88**b**	45.56**a**	39.95**a**	255.75**b**	228.35**a**	205.17**a**
	±40.91	±10.99	±29.80	±9.26	±1.42	±16.59	±25.18	±3.43	±16.59
Zn	129.56**b**	87.01**a**	111.09**ab**	24.97a	23.13a	17.45a	69.79**a**	98.99**c**	85.16**b**
	±19.06	±5.92	±11.04	±2.11	±1.40	±7.44	±6.87	±0.43	±1.60
Cu	11.47a	10.37a	13.12a	4.28a	5.36a	5.90a	14.72**a**	18.58**b**	18.66**b**
	±2.01	±2.54	±3.37	±0.47	±0.18	±2.01	±0.86	±1.21	±0.89
Mo	2.43a	2.08a	2.24a	0.25a	0.23a	0.21a	1.70**a**	2.18**ab**	2.42**b**
	±0.20	±0.51	±0.73	±0.01	±0.02	±0.12	±0.19	±0.20	±0.38

Note: The content of Na, Mg, Ca, K, Mn, Fe, Zn, Cu, Mo is expressed in μg DW^{-1} (±SE). Different letters (in bold) indicate differences in significance (one-way ANOVA) from 12, 6, 4 independent leaves, seeds and stems samples, respectively (Tukey test $p < 0.05$).

S7(B)); pre-treatment with lincomycin however did not enhance it further (Figure S7(C)). Notably, OE1 and OE2 do not show an altered sensitivity to photoinhibitory high light (not shown).

Progression of natural senescence is not associated with an increased activity of FDH promoter in *Vu* FDH::GUS *A. thaliana* plants grown either in control or in in calcareous soil (not shown). Again, FDH overexpression did not perturb natural senescence in *N. tabacum*; in fact, two hallmarks of senescence, i.e. reduction of chlorophyll content and of maximal photochemical efficiency F_v/F_m, occurred precociously in the oldest leaves of OE1 plants with respect to the wt leaves of same age, however such phenotype could not be confirmed in OE2 plants.

To test FDH involvement in the progression of dark-induced senescence (Tarantino et al. 2003; Barth et al. 2004; Luschin-Ebengreuth and Zechmann 2016) leaf disks from wt, OE1 and OE2 leaves (Figure 4(A)), were kept up to 12 days in darkness (Figure 4(B)) and total chlorophyll (Figure 4(C)), initial fluorescence F_0 (Figure 4(D)), maximal fluorescence F_m (Figure 4(E)) and maximal photochemical efficiency F_v/F_m (Figure 4(F)) were measured at different time points. After 5 d, the percentage of chlorophyll loss was higher in wt than in OE1 and OE2 disks (38%, 28% and 16% respectively). After 7 d, chlorophyll values were the same in all analysed lines, but several wt disks were already wilted; F_m and F_v/F_m parameters, measured on the remaining still turgid wt disks, were severely decreased (Figure 4(E, F)); no further measurements could be performed at time points later than 7 d, for wt disks. On the contrary, all OE1 and OE2 leaf disks appeared turgid during all time points and their photochemical parameters could be measured; the severe decrease in F_m and F_v/F_m values occur, in OE1 and OE2 disks, later than in wt disks, i.e. starting from 7 d onwards (Figure 4(E, F)).

To confirm a protective effect of FDH during dark induced senescence, the *A. thaliana* mutant *atfdh1-5* (Choi et al. 2014) carrying a T-DNA insertion in the third exon of the FDH gene At5g14780 (Figure S8(A, B)) was also analysed.

As expected, formate (0.4 mM or 1 mM) inhibits root elongation of both wt Col and *atfdh1-5* seedlings and the extent of such inhibition correlated with formate concentration (Figure S8(C)). Notably, *atfdh1-5* seedlings show shorter roots than wt in control condition already; this result suggests that the *atdfh1-5* mutant is not responding to formate treatment because of its lack of FDH activity, which is expected to cause a perturbation of the intracellular levels of formate; indeed, exogenous supply of formate has little effect in *atdfh1-5* roots (Figure S8(C)).

Col (wt) and *atfdh1-5* whole plants (Figure 5(A)) were kept up to 7 d at darkness, and fresh weight of plants rosettes (Figure 5(B)), chlorophyll content (Figure 5(C)), as well as F_v/F_m values (Figure 5(D)) were measured. *atfdh1-5* rosettes are smaller in weight, at all time points; their chlorophyll concentration, however, is not reduced, compared to wt values (Figure 5(C)). Lower F_v/F_m values are measured in *atfdh1-5* leaves with respect to wt (Figure 5(D)); however, after 24 h recovery at light, a faster increase of F_v/F_m is measured in *atfdh1-5* leaves (Figure 5(E)). A more pronounced decrease of F_v/F_m at darkness, in the *atfdh1-5* mutant, is also observed when the leaves are first detached from whole plants and then maintained in darkness (Figure S9(A)): after 4 d, *atfdh1-5* leaves appear slightly more chlorotic than wt (Figure S9(A)) and their F_v/F_m is lower than wt (Figure S9(B)). Again, after 24 h recovery at light, a faster increase of F_v/F_m in *atfdh1-5* mutant is observed (Figure S9(C)). After 7 d at darkness, all leaves are heavily affected (Figure S9(A, B)).

Discussion

Variations in the nutritional status of a single element trigger homeostatic adjustments involving the uptake, compartmentalization, trafficking and metabolic use of the other nutrients (Baxter et al. 2008a, 2008b; Baxter 2009; Vigani et al. 2017). These interactions constitute essential metabolic rearrangements aimed at optimizing the usage of nutritional resources (Vigani et al. 2017; Vigani and Murgia 2018). Various evidences suggested a link between Fe and Mo (Bittner and Mendel 2010; Bittner 2014), confirmed by biochemical, physiological and omics approaches applied to *C. sativus* plants grown under various Mo and/or Fe availability; the hypothetical scenarios for such interactions foresee FDH as one of the linking nodes (Vigani et al. 2017).

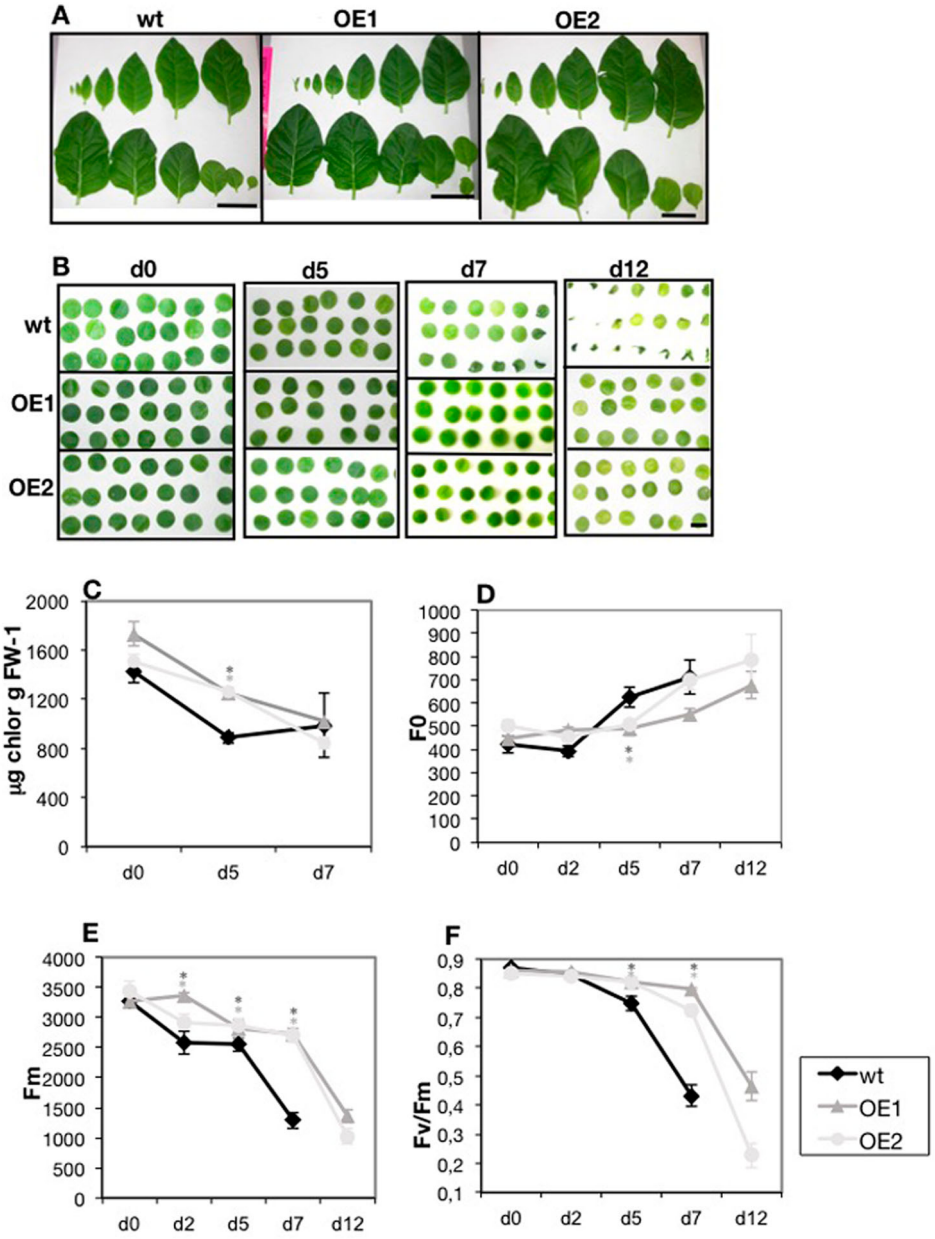

Figure 4. Dark-induced senescence in *N. tabacum* overexpressing lines OE1 and OE2. **(A)** Leaves detached from single 40 d old wt, OE1 and OE2 plants, aligned from youngest (up, left) to oldest (down, right). Bars = 10 cm. **(B)** leaf disks (6 mm in diameter) cut from the nr.1 to nr.6 youngest leaves in **(A),** after 0, 5, 7, 12 d in the dark. Bar = 6 mm. **(C)** total chlorophyll (µg chlorophyll g FW^{-1}) content after 0, 5, 7 d in the dark; **(D)** initial fluorescence F_0, **(E)** maximum fluorescence F_m, **(F)** F_v/F_m of leaf disks**,** after 0, 2, 5, 7,12 days in the dark. Each point in **(C)** is the mean value ± SE of three samples; each point in **(D, E, F)** is the mean value ± SE from ten samples. Asterisks in dark grey or light grey indicate statistically significant differences of OE1 and OE2 values with respect to wt, according to χ^2 test ($P <$ 0,001) (**C, D, E**) or to *T*-Test ($P < 0,05$) (**F**).

To investigate the role of FDH in modulating Mo-Fe homeostatic interactions, we first applied the bioinformatic approach of transcript correlation analysis. Such *in silico* analysis predicted a potential FDH involvement in the plant regulation of chlorophyll catabolism, senescence and responses against stress. Then, we took advantage of various genetic tools already available for the scientific community, in particular of a *A.thaliana* line stably transformed with *Vu* FDH::GUS construct (Lou et al. 2016). This line, together with *N.tabacum* lines overexpressing FDH (Lou et al. 2016) allowed the authors to successfully demonstrate that FDH confers tolerance to aluminium and low pH due to reduced formate production under Al or H^+ stress (Lou et al. 2016).

We used these lines to investigate the impact of FDH perturbation on plant ionome, and in particular of Mo and Fe plant nutritional status, as well as the relevance of FDH perturbation during dark-induced senescence.

Experimental results shown in the present work suggest that FDH promoter activity from *V.umbellata*, is Mo-dependent, at least when the construct is expressed in *A.thaliana*. This finding is noteworthy, since plant FDH is not itself an enzyme requiring the molybdenum cofactor MoCo, in contrast to its bacterial counterpart (Bittner and Mendel 2010; Bittner 2014). Notably, such Mo-dependent regulation of FDH expression was predicted in Vigani et al. (2017) from the results obtained with *C. sativus,* suggesting that the observed Mo-dependent regulation of FDH is indeed shared among different species. We could also observe an increased Mo content in OE1 and OE2 tobacco seeds overexpressing FDH suggesting that Mo content in seeds is dependent on a positive feedback loop between FDH activity and Mo.

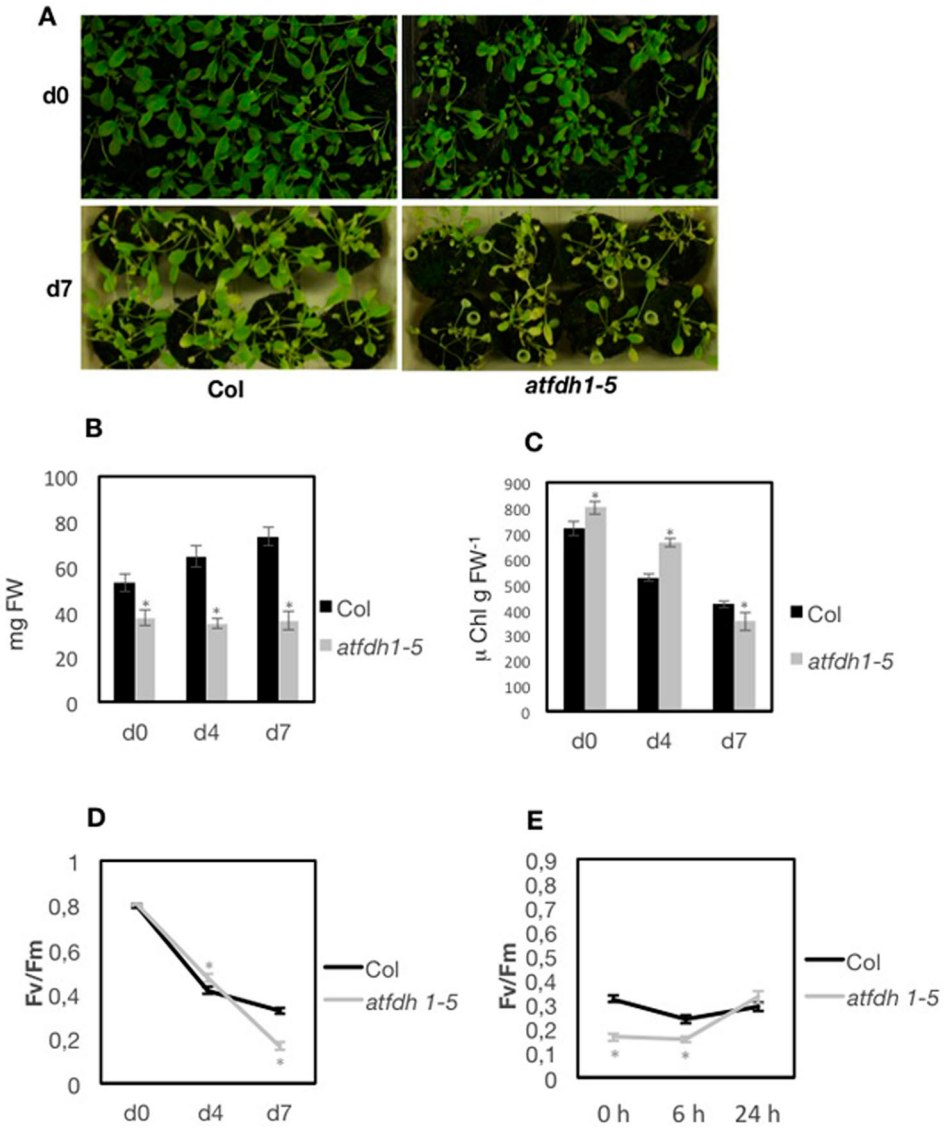

Figure 5. Dark-induced senescence in *atfdh1-5* whole plants. **(A)** three weeks old wt Col and *atfdh1-5* plants before light deprivation (day 0, upper panel) or after 7 d in darkness (d7, lower panel); **(B)** rosette weight (mg FW) and **(C)** total leaf chlorophyll (µg chlorophyll g FW^{-1}) of Col and *atfdh1-5* plants before light deprivation (d0), or after 4 or 7 d in darkness (d4, d7); bars in **(B)** and **(C)** are mean values ± SE from at least 8 independent samples each. **(D)** F_v/F_m of Col and *atfdh1-5* before light deprivation (d0), or after 4 or 7 d in darkness and **(E)** after 7 d in darkness followed by 6 h or 24 h recovery at light; each point in **(D)** and **(E)** is the mean value ± SE from at least 33 independent samples each. Asterisks in grey indicate statistically significant differences of *atfdh1-5* values, with respect to wt, according to χ^2 test ($P < 0{,}001$) (**B, C**) or *T*-test ($P < 0{,}05$) (**D, E**).

FDH OE1 and OE2 seeds have reduced Fe content and, accordingly, a slight but significant reduction of chlorophyll content is observed in OE1 and OE2 seedlings when grown under –Fe. These results indicate that the diminished Fe content in the OE tobacco lines still allows the plants to cope with the Fe nutritional demands in control conditions whereas it affects the plants when they are maintained under reduced Fe supply. Moreover, FDH OE seedlings show same chlorosis as wt (around 50% reduction of total chlorophyll content), when seedlings are grown under double Mo and Fe nutritional deficiency. This latter finding suggests that the impact of the simultaneous Mo and Fe nutritional deficiencies overcomes the altered Fe and Mo nutritional status of OE1 and OE2 seeds.

The transcript correlation analysis indicated a weak positive correlation of FDH with genes involved in C1 metabolism (e.g FTS, SHMT1, FALDH, FGH, MTR) (Song et al. 2013); on the contrary, FDH transcript shows a high correlation with two genes coding for chlorophyll catabolic enzymes, i.e. PaO and NYC1. The remaining chlorophyll catalyzing enzymes, i.e. SGR1, SGR2 and SGRL (Sakuraba et al. 2012, 2014), CLD1 and RCCR are not highly correlated with FDH. Moreover, FDH is highly correlated with NYC1 but not with its isozyme NOL (NYC1-like); these two enzymes are differently regulated and have different roles (Horie et al. 2009), NOL is indeed involved in the turnover of LHCII and the scavenging of free Chl b, whereas NYC1 activity is important for the degradation of Chl b under severe stress or during developmental transitions (Jia et al. 2015; Jibran et al. 2015). Notably, FDH transcript also shows a high correlation with other genes (e.g. BCM2) involved in chlorophyll homeostasis (Wang et al. 2020).

Both natural and dark-induced senescence are tightly regulated processes in plants; the progressive dismantling of various cellular components in senescing leaves is coordinated with the reallocation of various nutrients from senescing to younger leaves; any accumulation of potentially toxic molecules derived from chloroplast disassembly and degradations in senescing leaves, such as reactive chlorophyll catabolites and free Fe ions should be avoided (Hörtensteiner

and Kräutler 2011; Liebsch and Keech 2016; Luschin-Ebengreuth and Zechmann 2016; Woo et al. 2018). In particular, the Fe storage ferritin (Briat et al. 2010; Ramirez et al. 2011) takes part in both natural and dark-induced senescing programs (Tarantino et al. 2003; Murgia et al. 2007).

To validate the results obtained by analysis *in silico*, we monitored the effect of dark-induced senescence in both *N. tabacum* FDH OE lines and *A. thaliana atfdh1-5* mutant. Results confirm that indeed FDH is physiologically relevant for the onset of dark-induced senescence and also in the subsequent recovery phase, thus acting as protectant of the photochemical efficiency during dark-induced senescence and with opposite role during the recovery phase at light. These findings, in turn, might suggest that formate is noxious during the dark-phase and beneficial during the recovery phase at light. Next step in the understanding of the role of FDH in the dark induced senescence will be the analysis of the profile of chlorophyll catabolites in *atfdh* mutants, exposed to dark-induced senescence and during the recovery phase.

In conclusion, we show evidences that FDH, besides taking part in Fe and Mo homeostasis, is also relevant in the dark-induced senescing program; these findings reinforce the evidences of a tight coordination between senescence program and nutrient homeostasis.

Acknowledgement

We are grateful to Prof. Jian Li Yang for donating *A. thaliana* line *V. umbellata* FDH::GUS and *N. tabacum* 35S::VuFDH line1 and 35S::VuFDH line 2 (OE1 and OE2). *atfdh1-5* line Salk-108751 was generated by the Salk Institute and obtained through Nottingham Arabidopsis Stock Center (NASC). This research was supported by funds from the Italian National Ministry of Research (MIUR) PRIN 2017 – 2017FBS8YN_005 and MIUR FABBR 2017 and by local research funds of the Department of Life Sciences and Systems Biology (University of Turin).

Disclosure statement

No potential conflict of interest was reported by the author(s).

Funding

This work was supported by Ministero dell'Istruzione, dell'Università e della Ricerca [grant number 2017FBS8YN_005, FFABR18LCOLO_15]; the local research funds of the Department of Life Science and Systems Biology, University of Torino.

Notes on contributors

Irene Murgia is a plant physiologist at the Biosciences Department, Botanical Garden Città Studi, University of Milano, Italy; expert in plant nutrition and oxidative stress.

Gianpiero Vigani is a researcher at the Plant Physiology Unit of Department of Life Sciences and Systems Biology of the University of Turin, Italy; expertise in plant nutrition, plant metabolism and biochemistry, plant mitochondrial biology, plant-microbes interaction.

Dario Di Silvestre is a researcher at the Institute of Technologies for Biomedicine (ITB-CNR), Proteomics and Metabolomics Laboratory, Segrate, Italy; expert in bioinformatics and systems biology.

PierLuigi Mauri is a head of Proteomics and Metabolomics Laboratory at Institute of Technologies for Biomedicine (ITB-CNR), Segrate, Italy; expert in analytical biochemistry, mass spectrometry and proteomics.

Rossana Rossi is a researcher at Institute of Technologies for Biomedicine (ITB-CNR), Proteomics and Metabolomics Laboratory, Segrate, Italy; expert in mass spectrometry and proteomics.

Andrea Bergamaschi is a researcher at the Institute of Technologies for Biomedicine (ITB-CNR), Proteomics and Metabolomics Laboratory, Segrate, Italy; expert in mass spectrometry and proteomics.

Miriam Frisella is a former student at the Department of Biosciences, University of Milano, Italy.

Piero Morandini is a researcher in plant physiology at the University of Milano, Italy; expert in metabolic control analysis.

ORCID

Irene Murgia http://orcid.org/0000-0002-3193-6325
Gianpiero Vigani http://orcid.org/0000-0001-8852-3866
Dario Di Silvestre http://orcid.org/0000-0002-7143-6229
Pierluigi Mauri http://orcid.org/0000-0003-4364-0393
Rossana Rossi http://orcid.org/0000-0002-0313-7083
Andrea Bergamaschi http://orcid.org/0000-0003-4133-1917
Piero Morandini http://orcid.org/0000-0002-7994-6426

References

Abdel-Ghany SE, Ye H, Garifullina GF, Zhang L, Pilon-Smits EAH, Pilon M. 2005. Iron-sulfur cluster biogenesis in chloroplasts. Involvement of the scaffold protein CpIscA. Plant Physiol. 138:161–172.

Achkor H, Diaz M, Fernandez MR, Biosca JA, Pares X, Martinez MC. 2003. Enhanced formaldehyde detoxification by overexpression of glutathione-dependent formaldehyde dehydrogenase from *Arabidopsis*. Plant Physiol. 132:2248–2255.

Alberty RA, Cornish-Bowden A, Goldberg RN, Hammes GG, Tipton K, Westerhoff HV. 2011. Recommendations for terminology and databases for biochemical thermodynamics. Biophys Chem. 155:89–103.

Alekseeva AA, Savin SS, Tishkov VI. 2011. NAD+-dependent formate dehydrogenase from plants. Acta Naturae. 3:38–54.

Alonso JM, Stepanova AN, Leisse TJ, Kim CJ, Chen H, Shinn P, Stevenson DK, Zimmerman J, Barajas P, Cheuk R, et al. 2003. Genome-wide insertional mutagenesis of *Arabidopsis thaliana*. Science. 301:653–657.

Balk J, Pilon M. 2011. Ancient and essential: the assembly of the Fe-S clusters in plants. Trends Plant Sci. 16:218–226.

Barth C, Moeder W, Klessig DF, Conklin PL. 2004. The timing of senescence and response to pathogens is altered in the ascorbate-deficient *Arabidopsis* mutant vitamin c-1. Plant Physiol. 134:1784–1792.

Baxter I. 2009. Ionomics: studying the social network of mineral nutrients. Curr Opin Plant Biol. 12:381–386.

Baxter I, Muthukumar B, Park HC, Buchner P, Lahner B, Danku J, Zhao K, Lee J, Hawkesford MJ, Guerinot ML, et al. 2008a. Variation in molybdenum content across broadly distributed populations of *Arabidopsis thaliana* is controlled by a mitochondrial molybdenum transporter (MOT1). PLoS Genet. 4:e1000004.

Baxter I, Vitek O, Lahner B, Muthukumar B, Borghi M, Morrissey J, Guerinot ML, Salt DE. 2008b. The leaf ionome as a multivariable system to detect a plant's physiological status. Proc Natl Acad Sci USA. 105:12081–12086.

Binder BM, Walker JM, Gagne JM, Emborg TJ, Hemmann G, Bleecker AB, Vierstrab RD. 2007. The *Arabidopsis* EIN3 binding F-box proteins EBF1 and EBF2 have distinct but overlapping roles in ethylene signalling. Plant Cell. 19:509–523.

Bittner F. 2014. Molybdenum metabolism in plants and crosstalks to iron. Front Plant Sci. 5:28.

Bittner F, Mendel RR. 2010. Cell biology of molybdenum. In: Hell R, Mendel RR, editors. Cell biology of metals and nutrients. Plant Cell Monographs, 17. Berlin, Heidelberg: Springer-Verlag; p. 119–143.

Briat JF, Ravet K, Arnaud N, Duc C, Boucherez J, Touraine B, Cellier F, Gaymard F. 2010. New insights into ferritin synthesis and function highlight a link between iron homeostasis and oxidative stress in plants. Ann Bot. 105:811–822.

Burkhart SE, Lingard MJ, Bartel B. 2013. Genetic dissection of peroxisome-associated matrix protein degradation in *Arabidopsis thaliana*. Genetics. 193:125–141.

Bussell JD, Reichelt M, Wiszniewski AA, Gershenzon J, Smith SM. 2014. Peroxisomal ATP-binding cassette transporter COMATOSE and the multifunctional protein ABNORMAL INFLORESCENCE

MERISTEM are required for the production of benzoylated metabolites in *Arabidopsis* seeds. Plant Physiol. 164:48–54.
Chen H, Li S, Li L, Hu H, Zhao J. 2018. *Arabidopsis* EMB1990 encoding a plastid-targeted YlmG protein is required for chloroplast biogenesis and embryo development. Front Plant Sci. 16(9):181. doi:10.3389/fpls.2018.00181.
Chen LQ, Qu XQ, Hou BH, Sosso D, Osorio S, Fernie AR, Frommer WB. 2012. Sucrose efflux mediated by SWEET proteins as a key step for phloem loading. Science. 335:207–211.
Choi DS, Kim NH, Hwang BK. 2014. Pepper mitochondrial formate dehydrogenase1 regulates cell death and defence responses against bacterial pathogen. Plant Physiol. 166:1298–1311.
Cotton CAR, Edlich-Muth C, Bar-Even A. 2018. Reinforcing carbon fixation: CO2 reduction replacing and supporting carboxylation. Curr Opin Biotechnol. 49:49–56.
Couturier J, Touraine B, Briat JF, Gaymard F, Rouhier N. 2013. The iron-sulfur cluster assembly machineries in plants: current knowledge and open questions. Front Plant Sci. 4:259. doi:10.3389/fpls.2013.00259.
Cui MH, Ok SH, Yoo KS, Jung KW, Yoo SD, Shin JS. 2013. An *Arabidopsis* cell growth defect factor-related protein, CRS, promotes plant senescence by increasing the production of hydrogen peroxide. 2013. Plant Cell Physiology. 54:155–167. doi:10.1093/pcp/pcs161.
Dong T, Xu ZY, Park Y, Kim DH, Lee Y, Hwang I. 2014. Abscisic acid uridine diphosphate glucosyltransferases play a crucial role in abscisic acid homeostasis in *Arabidopsis*. Plant Physiol. 165:277–289.
Douglas SE, Penny SL. 1999. The plastid genome of the cryptophyte alga *Guillarda theta*: complete sequence and conserved synteny groups confirm its common ancestry with red algae. J Mol Evol. 48:236–244.
Elorza A, Leon G, Gomez I, Mouraz A, Holuigue L, Araya A, Jordana X. 2004. Nuclear SDH2-1 and SDH2-2 genes, encoding the iron-sulfur subunit of mitochondrial complex II in *Arabidopsis*, have distinct cell-specific expression patterns and promoter activities. Plant Physiol. 136:4072–4087.
Foster J, Kim HU, Nakata PA, Browse J. 2012. A previously unknown oxalyl-CoA synthetase is important for oxalate catabolism in *Arabidopsis*. Plant Cell. 24:1217–1229.
Fukusaki EI, Ikeda T, Shiraishi T, Nishizawa T, Kobayashi A. 2000. Formate dehydrogenase gene of *Arabidopsis thaliana* is induced by formaldehyde and not by formic acid. J Biosci Bioeng. 90:691–693.
Herman PL, Ramberg H, Baack RD, Markwell J, Osterman JC. 2002. Formate dehydrogenase in *Arabidopsis thaliana*: overexpression and subcellular localization in leaves. Plant Sci. 163:1137–1145.
Horie Y, Ito H, Kusaba M, Tanaka R, Tanaka A. 2009. Participation of chlorophyll b reductase in the initial step of the degradation of light-harvesting chlorophyll a/b-protein complexes in *Arabidopsis*. J Biol Chem. 284:17449–17456.
Hörtensteiner S. 2013. Update on the biochemistry of chlorophyll breakdown. Plant Mol Biol. 82:505–517.
Hörtensteiner S, Kräutler B. 2011. Chlorophyll breakdown in higher plants. Biochim Biophys Acta. 1807:977–988.
Hourton-Cabassa C, Ambard-Bretteville F, Moreau F, Davy de Virville J, Remy R, Colas des Francs-Small C. 1998. Stress induction of mitochondrial formate dehydrogenase in potato leaves. Plant Physiol. 116:627–635.
Islam M, Maffei EM, Vigani G. 2020. The geomagnetic field is a contributing factor for an efficient Fe uptake in *Arabidopsis thaliana*. Front Plant Sci. 11:325. doi:10.3389/fpls.2020.00325.
Itai RN, Ogo Y, Kobayashi T, Nakanishi H, Nishizawa NK. 2013. Rice genes involved in phytosiderophore biosynthesis are synchronously regulated during the early stages of iron deficiency in roots. Rice. 6:16. doi:10.1186/1939-8433-6-16.
Jia T, Ito H, Hu X, Tanaka A. 2015. Accumulation of the NON-YELLOW COLORING1 protein of the chlorophyll cycle requires chlorophyll b in *Arabidopsis thaliana*. Plant J. 81:586–596.
Jibran R, Sullivan KL, Crowhurst R, Erridge ZA, Chagnè D, McLachlan ARG, Brummell DA, Dijkwel PP, Hunter DA. 2015. Staying green postharvest: how three mutations in the *Arabidopsis* chlorophyll b reductase gene NYC1 delay degreening by distinct mechanisms. J Exp Bot. 66:6849–6862.
Kabeya Y, Nakanishi H, Suzuki K, Ichikawa T, Kondou Y, Matsui M, Miyagishima S. 2010. The Ylm G protein has a conserved function related to the distribution of nucleoids in chloroplasts and cyanobacteria. BCM Plant Biology. 10:57.
Kobayashi T, Nishizawa NK. 2012. Iron uptake, translocation, and regulation in higher plants. Annu Rev Plant Biol. 63:131–152.
Kobayashi T, Suzuki M, Inoue H, Itai RN, Takahashi M, Nakanishi H, Mori S, Nishizawa NK. 2005. Expression of iron-acquisition-related genes in iron-deficient rice is co-ordinately induced by partially conserved iron-deficiency-responsive elements. J Exp Bot. 56:1305–1316.
Kräutler B. 2016. Breakdown of chlorophyll in higher plants-Phyllobilins as abundant, yet hardly visible signs of ripening, senescence and cell death. Angew Chem. 55:4882–4907.
Le Hir R, Spinner L, Klemens PAW, Chakraborti D, de Marco F, Vilaine F, Wolff N, Lemoine R, Porcheron B, Géry C, et al. 2015. Disruption of the sugar transporters AtSWEET11 and AtSWEET12 affects vascular development and freezing tolerance in *Arabidopsis*. Mol Plant. 8:1687–1690.
Li R, Bonham-Smith PC, King J. 2001. Molecular characterization and regulation of formate dehydrogenase in *Arabidopsis thaliana*. Can J Bot. 79:796–804. doi:10.1139/b01-056.
Liebsch D, Keech O. 2016. Dark-induced leaf senescence: new insights into a complex light-dependent regulatory pathway. New Phytol. 212:563–570.
Lou HQ, Gong YL, Fan W, Xu JM, Liu Y, Cao MJ, Wang MH, Yang JL, Zheng SJ. 2016. A formate dehydrogenase confers tolerance to aluminum and low pH. Plant Physiol. 171:294–305.
Luschin-Ebengreuth N, Zechmann B. 2016. Compartment-specific investigations of antioxidants and hydrogen peroxide in leaves of *Arabidopsis thaliana* during dark-induced senescence. Acta Physiol Plant. 38:133. doi:10.1007/s11738-016-2150-6.
Maia LB, Fonseca L, Moura I, Moura JJ. 2016. Reduction of carbon dioxide by a molybdenum-containing formate dehydrogenase: a kinetic and mechanistic study. J Am Chem Soc. 138:8834–8846.
Majeran W, Friso G, Asakura Y, Qu X, Huang M, Ponnala L, Watkins KP, Barkan A, van Wijk KJ. 2012. Nucleoid-enriched proteome in developing plastids and chloroplasts from maize leaves: a new conceptual framework for nucleoid functions. Plant Physiol. 158:156–189.
Martin-Sanchez L, Ariotti C, Garbeva P, Vigani G. 2020. Investigating the effect of below ground microbial volatiles on plant nutrient status: perspective and limitations. J Plant Interact. 5(1):188–195. doi:10.1080/17429145.2020.1776408.
McNeilly D, Schofield A, Stone SL. 2018. Degradation of the stress-responsive enzyme formate dehydrogenase by the RING-type E3 ligase Keep on Going and the ubiquitin 26S proteasome system. Plant Mol Biol. 96:265–278. doi:10.1007/s11103-017-0691-8.
Menges M, Dóczi R, Ökrész L, Morandini P, Mizzi L, Soloviev M, Murray JAH, Bögre L. 2008. Comprehensive gene expression atlas for the *Arabidopsis* MAP kinase signalling pathways. New Phytol. 179:643–662.
Mishra B, Sun Y, Ahmed H, Liu X, Mukhtar MS. 2017. Global temporal dynamic landscape of pathogen-mediated subversion of *Arabidopsis* innate immunity. Sci Rep. 7:7849. doi:10.1038/s41598-017-08073-z.
Miyazaki JH, Yang SF. 1987. The methionine salvage pathway in relation to ethylene and polyamine biosynthesis. Physiol Plant. 69:366–370.
Murata N, Allakhverdiev SI, Nishiyama Y. 2012. The mechanism of photoinhibition in vivo: Re-evaluation of the roles of catalase, α-tocopherol, non-photochemical quenching, and electron transport. Biochim Biophys Acta. 1817:1127–1133.
Murgia I, Giacometti S, Balestrazzi A, Paparella S, Pagliano C, Morandini P. 2015. Analysis of the transgenerational iron deficiency stress memory in *Arabidopsis thaliana* plants. Front Plant Sci. 6:745. doi:10.3389/fpls.2015.00745.
Murgia I, Morandini P, Moroni A, Soave C. 1998. A non-destructive selection method for resistance to fusicoccin in *Arabidopsis thaliana*. Plant Cell Rep. 18:255–259. doi:10.1007/s002990050567.
Murgia I, Tarantino D, Soave C, Morandini P. 2011. Arabidopsis CYP82C4 expression is dependent on Fe availability and circadian rhythm, and correlates with genes involved in the early Fe deficiency response. J Plant Physiol. 168:894–902. doi:10.1016/j.jplph.2010.11.020.
Murgia I, Vazzola V, Tarantino D, Cellier F, Ravet K, Briat JF, Soave C. 2007. Knock-out of the ferritin *AtFer1* causes earlier onset of age-dependent leaf senescence in *Arabidopsis*. Plant Physiol Biochem. 45:898–907.
Murgia I, Vigani G. 2015. Analysis of *Arabidopsis thaliana atfer4-1, atfh and atfer4-1/atfh* mutants uncovers frataxin and ferritin contributions to leaf ionome homeostasis. Plant Physiol Biochem. 94:65–72.

Oldenburg DJ, Bendich AJ. 2015. DNA maintenance in plastids and mitochondria of plants. Front Plant Sci. 6:883.

Pfalz J, Pfanneschmidt T. 2013. Essential nucleoid proteins in early chloroplast development. Trends Plant Sci. 18:186–194.

Prabhu V, Chatson KB, Lui H, Abrams GD, King J. 1996. ^{13}C nuclear magnetic resonance detection of interaction of serine hydroxymethyltransferase with C1-tetrahydrofolate synthase and glycine decarboxylase complex activities in *Arabidopsis*. Plant Physiol. 112:8713–8719.

Rajniak J, Giehl RF, Chang E, Murgia I, von Wirén N, Sattely ES. 2018. Biosynthesis of redox-active metabolites as a general strategy for iron acquisition in plants. Nature Chem Biol. 14(5):442–450. doi:10.1038/s41589-018-0019-2.

Ramirez L, Simontacchi M, Murgia I, Zabaleta E, Lamattina L. 2011. Nitric oxide, Nitrosyl iron complexes, ferritin and frataxin: a well-equipped team to preserve plant iron homeostasis. Plant Sci. 181:582–592.

Sakuraba Y, Park SY, Kim YS, Wang SH, Yoo SC, Hoertensteiner S, Paek NC. 2014. *Arabidopsis* STAY-GREEN2 is a negative regulator of chlorophyll degradation during leaf senescence. Mol Plant. 7:1288–1302.

Sakuraba Y, Schelbert S, Park SY, Han SH, Lee BD, Besagni Andres C, Kessler S, Paek NC. 2012. STAY-GREEN and chlorophyll catabolic enzymes interact at light-harvesting complex II for chlorophyll detoxification during leaf senescence in *Arabidopsis*. Plant Cell. 24:507–518.

Schuler MA, Duan H, Bilgin M, Ali S. 2006. *Arabidopsis* cytochrome P450s through the looking glass: a window on plant biochemistry. Phytochem Rev. 5:205–237.

Schwacke R, Schneider A, Van Der Graaff E, Fischer K, Catoni E, Desimone M, Frommer WB, Flügge UI, Kunze R. 2003. ARAMEMNON, a novel database for *Arabidopsis* integral membrane proteins. Plant Physiol. 131:16–26.

Shiraishi T, Fukusaki E, Miyake C, Yokota A, Kobayashi A. 2000. Formate protects photosynthetic machinery from photoinhibition. J Biosci Bioeng. 89:564–568.

Song ZB, Xiao SQ, You L, Wang SS, Tan H, Zhi K, Chen LM. 2013. C1 metabolism and the Calvin cycle function simultaneously and independently during HCHO metabolism and detoxification in A*rabidopsis thaliana* treated with HCHO solutions. Plant Cell Environ. 36:1490–1506.

Sugliani M, Abdelkefi H, Ke H, Bouveret E, Robaglia C, Caffarri S, Field B. 2016. An ancient bacterial signaling pathway regulates chloroplast function to influence growth and development in *Arabidopsis*. Plant Cell. 28:661–679.

Tarantino D, Petit JM, Lobreaux S, Briat JF, Soave C, Murgia I. 2003. Differential involvement of the IDRS cis-element in the developmental and environmental regulation of the AtFer1 ferritin gene from *Arabidopsis*. Planta. 217:709–716. doi:10.1007/s00425-003-1038-z.

Tarantino D, Vannini C, Bracale M, Campa M, Soave C, Murgia I. 2005. Antisense reduction of thylakoidal ascorbate peroxidase in *Arabidopsis* enhances Paraquat-induced photooxidative stress and nitric oxide-induced cell death. Planta. 221:757–765. doi:10.1007/s00425-005-1485-9.

Tyystjärvi E, Aro EM. 1996. The rate constant of photoinhibition, measured in lincomycin-treated leaves, is directly proportional to light intensity. Proc Natl Acad Sci USA. 93:2213–2218.

Urzica EI, Casero D, Yamasaki H, Hsieh SI, Adler LN, Karpowicz SJ, Blaby-Haas CE, Clarke SG, Loo JA, Pellegrini M, Merchant SS. 2012. Systems and trans-system level analysis identifies conserved iron deficiency responses in the plant lineage. Plant Cell. 24:3921–3948.

van der Biezen EA, Sun J, Coleman M, Bibb MJ, Jones JDG. 2000. *Arabidopsis* rela/SpoT homologs implicate (p)ppGpp in plant signaling. Proc Natl Acad Sci USA. 97:3747–3752.

Vigani G, Di Silvestre D, Agresta AM, Donnini S, Mauri P, Gehl C, Bittner F, Murgia I. 2017. Molybdenum and iron mutually impact their homeostasis in cucumber (*Cucumis sativus* L.) plants. New Phytol. 213:1222–1241.

Vigani G, Murgia I. 2018. Iron-Requiring enzymes in the Spotlight of Oxygen. Trends Plant Sci. 23:874–882. doi:10.1016/j.tplants.2018.07.005.

Wang P, Richter AS, Kleeberg JRW, Geimer S, Grimm B. 2020. Post-translational coordination of chlorophyll biosynthesis and breakdown by BCMs maintains chlorophyll homeostasis during leaf development. Nat Commun. 11:1254. doi:10.1038/s41467-020-14992-9.

Weber P, Fulgosi H, Piven I, Müller I, Krupinska K, Duong VH, Herrmann RG, Sokolenkno A. 2006. TCP34, a nuclear-encoded response regulator-like TPR protein of higher plant chloroplasts. J Mol Biol. 357:535–549. doi:10.1016/j.jmb.2005.12.079.

Woo HR, Masclaux-Daubresse C, Lim PO. 2018. Plant senescence: how plants know when and how to die. J Exp Bot. 69:715–718. doi:10.1093/jxb/ery011.

Yabe T, Nakai M. 2006. *Arabidopsis* AtIscA-I is affected by deficiency of Fe-S cluster biosynthetic scaffold AtCnfU-V. Biochem Biophys Res Commun. 340:1047–1052.